



Enhanced photoluminescence of $\text{BaMgAl}_{10}\text{O}_{17}:\text{Eu}^{2+}$ nanophosphor for PDP application

Zhaofeng Wang^a, Yuhua Wang^{a,b,*}, Yezhou Li^a, Bitao Liu^a

^a Department of Materials Science, School of Physical Science and Technology, Lanzhou University, Lanzhou 730000, People's Republic of China

^b Key Laboratory for Magnetism and Magnetic Materials of the Ministry of Education, Lanzhou University, Lanzhou 730000, People's Republic of China

ARTICLE INFO

Article history:

Received 20 May 2010

Received in revised form 3 September 2010

Accepted 3 September 2010

Available online 21 September 2010

Key words:

Nanophosphor

Optical properties

Luminescence

ABSTRACT

$\text{BaMgAl}_{10}\text{O}_{17}:\text{Eu}^{2+}$ nanorods were synthesized by sol–gel technique, and their luminescent properties were investigated upon the irradiation of vacuum ultraviolet (VUV) light. By introducing surfactant cetyltri-methyl-ammonium bromide (CTAB) in sol–gel process and additional Mg^{2+} in the raw materials, the emission intensity and thermal stability of the nanophosphor were both enhanced. The above improvements made it possible that the nanosized BAM phosphor could be a good alternative for PDP application.

© 2010 Elsevier B.V. All rights reserved.

1. Introduction

$\text{BaMgAl}_{10}\text{O}_{17}:\text{Eu}^{2+}$ (BAM) has been regarded as the best blue-emitting phosphor for fluorescent lamps, plasma display panels (PDPs) and Hg-free lamps due to its high luminance efficiency and good color purity under ultraviolet (UV) and vacuum ultraviolet (VUV) excitation [1]. Recently, intense research activity has been focused on nanoscaled BAM phosphor since it is beneficial to obtain the miniature display device with higher resolution [2–4]. However, the emission intensity of the current BAM nanophosphor is much lower than that of the bulk, and it still suffers from the degradation during the baking process in PDP manufacturing, which would greatly reduce the emission efficiency of BAM phosphor [5,6]. Therefore, further improvements are necessary for nanosized BAM.

In our previous work [7], BAM nanorods with good size distribution were successfully synthesized by sol–gel method. But the VUV luminescent intensity of the nanophosphor is only about 78.15% of that of the commercial BAM phosphor (Kx-501). In the systems of ZnO and $\text{ZnSiO}_4:\text{Mn}$, it was found that the addition of cetyltri-methyl-ammonium bromide (CTAB) in sol–gel process could improve their luminescent intensity attributing to the interaction between CTA^+ and anionic group [8–11]. Moreover, the doping of Mg^{2+} to substitute Al^{3+} in the bulk BAM could effectively restrain

the thermal degradation [12]. Hence in this work, we synthesized Mg^{2+} doped $\text{BaMgAl}_{10}\text{O}_{17}:\text{Eu}^{2+}$ nanophosphor by CTAB assisted sol–gel technique, and explored its photoluminescence under VUV excitation.

2. Experimental

The starting materials Eu_2O_3 (99.99%), $\text{Al}(\text{NO}_3)_3 \cdot 9\text{H}_2\text{O}$ (99.0%), $\text{Ba}(\text{NO}_3)_2$ (99.5%) and $\text{Mg}(\text{NO}_3)_2 \cdot 6\text{H}_2\text{O}$ (99.0%) were weighted as the nominal composition of $\text{Ba}_{0.9}\text{Mg}(\text{Al}_{1-x}\text{Mg}_x)_{10}\text{O}_{17-5x}:\text{Eu}^{2+}$. Then, citric acid with a 2:1 mole of citric acid to Al^{3+} ratio were dissolved in deionized water and the pH value was adjusted to 3 by $\text{NH}_3 \cdot \text{H}_2\text{O}$. And then a stoichiometric amount of starting materials was dissolved in the citric solution. After that, CTAB was added in the solution with stirring about half an hour. Subsequently, the pH value of the solution was adjusted to 5 and heated to 60 °C with ceaselessly stirring for half an hour to gain the sol. The sol was placed in room temperature for about 40 min in succession. Then it was dried in a muffle oven at 120 °C, and the volume of the gel expanded greatly and the puffy and porous dried gel was obtained. After the gel was ground in an agate mortar, it was sintered at 1000 °C for 2 h in air and at 1300 °C for 4 h in a reducing atmosphere (5% H_2/N_2 gas mixture).

The X-ray diffraction (XRD) patterns were obtained on a Rigaku D/max-2400 X-ray diffractometer. The morphology of the powders was examined by transmission electron microscopy (TEM) with a Hitachi H-800 transmission electron microscope using an accelerating voltage of 100 kV. The emission spectra were measured by FLS-920T fluorescence spectrophotometer with a VM-504-type vacuum monochromator. All measurements were carried out at room temperature.

3. Results and discussion

The crystallinity and phase purity of the as-prepared samples were examined by XRD. Fig. 1 gives the typical XRD patterns of $\text{Ba}_{0.9}\text{Mg}(\text{Al}_{0.96}\text{Mg}_{0.04})_{10}\text{O}_{16.8}:\text{Eu}^{2+}$ phosphor synthesized by sol–gel process with 2% CTAB added. The diffraction peaks can be indexed and match well with JCPDs file of BAM (Joint Committee

* Corresponding author at: Department of Materials Science, School of Physical Science and Technology, Lanzhou University, Lanzhou 730000, People's Republic of China. Tel.: +86 931 8912772; fax: +86 931 8913554.

E-mail address: wylh@lzu.edu.cn (Y. Wang).

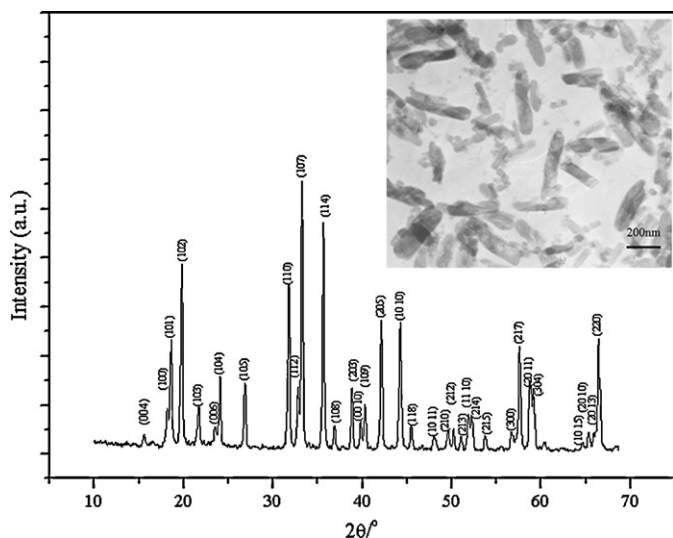


Fig. 1. Typical XRD patterns of $\text{Ba}_{0.9}\text{Mg}(\text{Al}_{0.96}\text{Mg}_{0.04})_{10}\text{O}_{16.8}:0.1\text{Eu}^{2+}$ phosphor synthesized by sol-gel process with 2% CTAB added; the inset is the TEM image of the sample.

for Power Diffractions Standards, No. 26-0163). The result indicates that the sample is pure phase, which have β -alumina structure corresponding to the space group $\text{P}6_3/\text{mmc}$. All of the other samples doped with different concentration of CTAB and Mg^{2+} are also characterized to be single phase. On the contrary for sol-gel technique, the presence of intermediate which brought on impurities in the product was identified in conventional solid-state reaction even at the temperature of 1600°C [13].

The microstructure of the particle was revealed by TEM. The typical TEM image of the sample (doped with 4% Mg and 2% CTAB) is shown in the inset of Fig. 1. It exhibits rod-like morphology with the size of 50–100 nm in diameter and 300 nm in length. The particles are homogeneous, which could be convenient to coat the panel during the manufacture of PDPs [11].

Fig. 2 shows the emission spectrum of BAM nanorods doped with 2% CTAB ($\lambda_{\text{ex}} = 147 \text{ nm}$). The emission spectrum presents a broad band locating at about 452 nm, which attributes to the

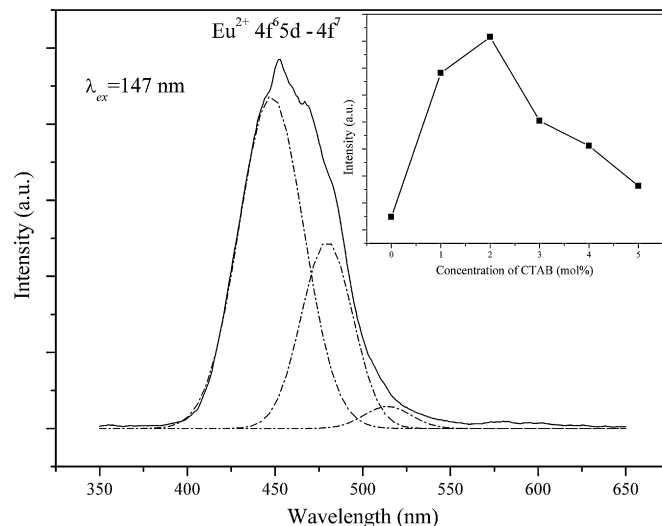


Fig. 2. Emission spectrum of BAM nanorods doped with 2% CTAB by 147 nm excitation; the inset is the relative emission intensity of the nanophosphors with different concentration of CTAB.

$4f^65d \rightarrow 4f^7(^8S_{7/2})$ transition of Eu^{2+} [14]. The band is of asymmetrical distribution which relates to the different sites that Eu^{2+} occupy in BAM. By Gaussian fitting the VUV emission spectrum, three peaks are found locating at 446 nm, 477 nm and 517 nm, respectively, corresponding to the emission of Eu^{2+} in the sites of BR, a-BR and spinel layer [15–17]. To probe into the influence of CTAB on VUV emission intensity, the luminescent properties of the nanorods with different concentration of CTAB are depicted under 147 nm excitation. From the inset of Fig. 2, it can be seen that the addition of CTAB evidently enhances the relative intensity of the nanophosphor. The optimum concentration of CTAB is determined to be 2%, which heightens the original emission intensity about 16%. This phenomenon could be interpreted by the inherent function of the surfactant CTAB; it could not only reduce the surface tension of solution and lower the energy to form a new phase, but also eliminate the defect states through chemical interaction between surfactants and inorganic species during the synthesis [8–10].

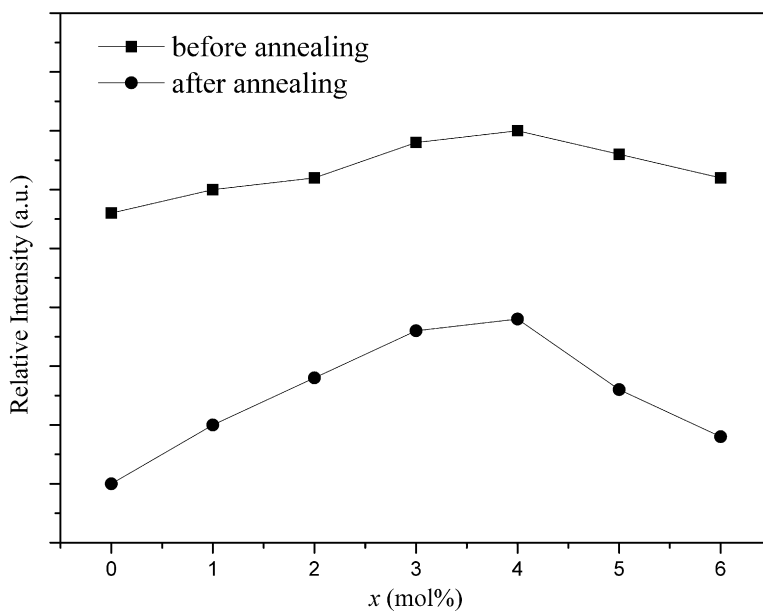


Fig. 3. Relative emission intensity of $\text{Ba}_{0.9}\text{Mg}(\text{Al}_{1-x}\text{Mg}_x)_{10}\text{O}_{17-5x}:0.1\text{Eu}^{2+}$ ($0 \leq x \leq 0.06$) nanophosphors synthesized by % CTAB assisted sol-gel technique before and after annealing ($\lambda_{\text{ex}} = 147 \text{ nm}$).

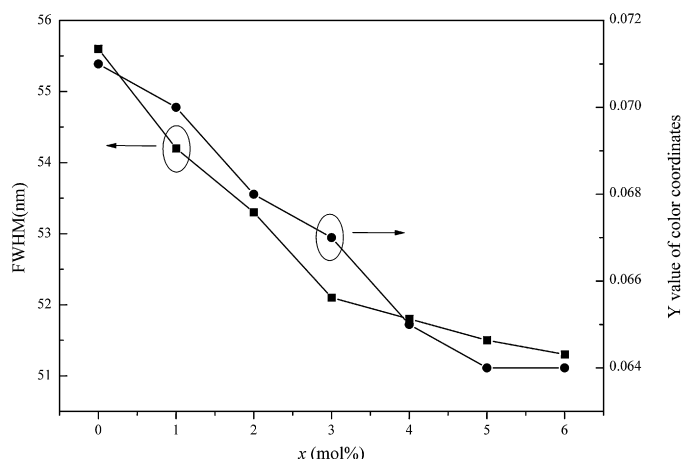


Fig. 4. FWHM and y value of color coordinates of the samples synthesized with 2% CTAB and different concentration of Mg^{2+} .

As we know, the blue phosphor BAM could be jeopardized by the thermal degradation when heated at about 550°C . The relative emission intensity of the above CTAB-prepared nanorods is valued after a heat-treatment of 550°C for 1 h in air condition. Their deterioration ratios are 25.3% (0% CTAB), 24.4% (2% CTAB), 24.9% (4% CTAB) and 25.5% (6% CTAB), respectively. So the addition of CTAB in the sol-gel process does not affect the thermal stability of the BAM nanorods.

For the purpose of getting BAM nanophosphor with high emission intensity and good thermal stability, Mg^{2+} was introduced in the host on the basis of adding 2% CTAB. Fig. 3 presents the relative emission intensity of BAM nanophosphors with the variation of doping Mg^{2+} before and after annealing ($\lambda_{\text{ex}} = 147 \text{ nm}$). It can be obviously found that the addition of Mg^{2+} in the sites of Al^{3+} could further enhance the emission intensity of BAM nanophosphor before and after annealing. The optimum concentration of Mg^{2+} is 4%. On one hand, due to Mg–O has absorption in VUV region, the doping of additional Mg^{2+} could enhance the emission intensity of BAM phosphor [11]. On the other hand, since the substitution of Mg^{2+} for Al^{3+} is a substitution of lower valence cations for higher valence cations, considering the charge compensating mechanism, anion vacancies or interstitial cations must be generated in the beta alumina structure. These defects play roles on the quenching centers and decrease the emission intensity. As a result, the optimum doping concentration of Mg^{2+} is affected by the above two reasons. The thermal degradation of the optimum nanophosphor (with the addition of 2% CTAB and 4% Mg) is calculated to be 18.5%, which may be compared to a value of 6% with a nanophosphor synthesized with only 2% CTAB.

To analyze the improvement of the thermal stability, the changes of full-width at half-maximum (FWHM) and y value of color coordinates of the samples synthesized with 2% CTAB and different concentrations of Mg^{2+} are shown in Fig. 4. As mentioned in Fig. 2(a), the emission spectrum of BAM is composed of three emission bands which correspond to Eu^{2+} in different sites of Ba^{2+} . With the variation of the distribution of Eu^{2+} in the three sites, the color coordinates and FWHM could change synchronously. As a result, the variations in Fig. 4 reflect the lattice environment of Eu^{2+} is changed by doping Mg^{2+} . The y value of the emissions for Eu^{2+} in three sites is different that it decreases with decreasing wavelength. Therefore, the decrease of y value with increasing the doping concentration of Mg^{2+} (as shown in Fig. 4) indicates that Eu^{2+} migrate from the sites emitting long wavelength (spinel block) to those emitting short wavelength (mirror layer). Associated with the consideration that the migration of Eu^{2+} in BAM from mirror planes to spinel blocks is another essential mechanism of the ther-

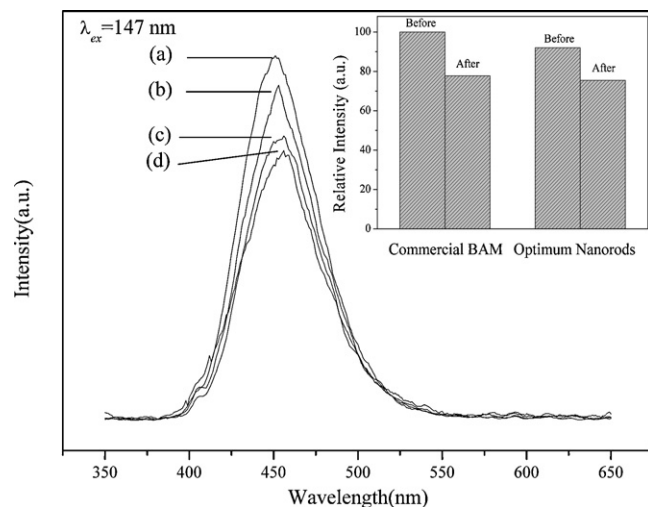


Fig. 5. Emission spectra of BAM samples: (a) commercial phosphor, before annealing, (b) optimum nanorods, before annealing, (c) commercial phosphor, after annealing, and (d) optimum nanorods, after annealing ($\lambda_{\text{ex}} = 147 \text{ nm}$); the inset is the columnar graph of the emission intensity.

mal degradation besides the oxidation of Eu^{2+} to Eu^{3+} [18], the introduction of Mg^{2+} to substitute Al^{3+} will certainly improve its thermal stability.

Therefore, the optimum nanoscaled BAM is that synthesized by 2% CTAB assisted sol-gel method with 4% Mg^{2+} doped. The comparison between the optimum nanorods and commercial BAM phosphor (Kx-501) on emission intensity and thermal stability are illustrated in Fig. 5 ($\lambda_{\text{ex}} = 147 \text{ nm}$). Before annealing, the luminescence intensity of the nanorods is nearly 92% of that of the commercial phosphor. After annealing, the luminescence intensity of the nanorods is nearly 97% of that of the annealed commercial phosphor. These data reflect that the thermal stability of the nanorods is superior to that of the commercial phosphor.

4. Conclusions

$\text{Ba}_{0.9}\text{Mg}(\text{Al}_{1-x}\text{Mg}_x)_{10}\text{O}_{17-5x}:0.1\text{Eu}^{2+}$ nanorods were synthesized by CTAB assisted sol-gel method. The emission intensity and thermal stability of the nanorods under 147 nm excitation were successfully enhanced through introducing CTAB and additional Mg^{2+} . The optimum BAM nanorods approached to the commercial blue phosphor on emission intensity, and exhibited better thermal stability than the latter. All of the results indicated that the BAM nanorods could be potentially applied in high resolution plasma display panels.

Acknowledgements

The authors would like to thank the National Natural Science Foundation of China (10874061), the Research Fund for the Doctoral Program of Higher Education (200807300010) and the National Science Foundation for Distinguished Young Scholars (50925206).

References

- [1] T. Jüstel, J.C. Krupa, D.U. Wiechert, J. Lumin. 93 (2001) 179.
- [2] Z. Chen, Y. Yan, J. Liu, Y. Yin, H. Wen, J. Zao, D. Liu, H. Tian, C. Zhang, S. Li, J. Alloys Compd. 473 (2009) L13.
- [3] D.-K. Kim, S.-H. Hwang, I.-G. Kim, J.-C. Park, S.-H. Byeon, J. Solid State Chem. 178 (2005) 1414.
- [4] C. Panatarani, I. Wuled Lenggoro, N. Itoh, H. Yoden, K. Okuyama, Mater. Sci. Eng. B 122 (2005) 188.

- [5] S. Oshio, T. Matsuoka, S. Tanaka, H. Kobayashi, *J. Electrochem. Soc.* 145 (1998) 3903.
- [6] K. Sohn, S. Kim, H. Park, *Appl. Phys. Lett.* 81 (2002) 1759.
- [7] Z. Wang, Y. Wang, B. Liu, *J. Nanosci. Nanotechnol.* 10 (2010) 2177.
- [8] N. Kim, S. Choi, H.J. Lee, K.J. Kim, *Curr. Appl. Phys.* 9 (2009) 3.
- [9] F. Li, L. Hu, Z. Li, X. Huang, *J. Alloys Compd.* 465 (2008) L14.
- [10] Y. Xu, Z. Ren, G. Cao, W. Ren, K. Deng, Y. Zhong, *Mater. Lett.* 62 (2008) 4525.
- [11] X. Yu, Y. Wang, *J. Phys. Chem. Solids* 70 (2009) 1146.
- [12] Z.H. Zhang, Y.H. Wang, *Mater. Lett.* 61 (2007) 4128.
- [13] S. Oshio, K. Kitamura, T. Shigeta, S. Horii, T. Matsuoka, S. Tanaka, H. Kobayashi, *J. Electrochem. Soc.* 146 (1999) 392.
- [14] G. Blasse, B.C. Geiabmaier, *Luminescent Materials [M]*, Springer-Verlag, Berlin, 1994, pp. 28–30.
- [15] P. Boolchand, K.C. Mishra, M. Raukas, A. Ellens, P.C. Schmidt, *Phys. Rev. B* 66 (2002) 134429.
- [16] K.C. Mishra, M. Raukas, A. Ellens, K.H. Johnson, *J. Lumin.* 96 (2002) 95.
- [17] C.R. Ronda, B.M.J. Smets, *J. Electrochem. Soc.* 136 (1989) 570.
- [18] Z.H. Zhang, Y.H. Wang, X.X. Li, *J. Alloys Compd.* 478 (2009) 801.